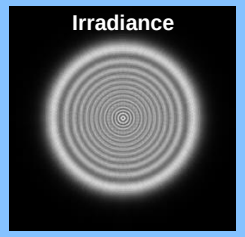

Image intensity

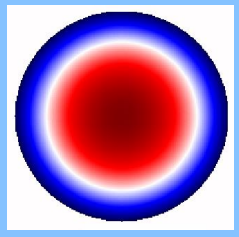

Wavefront phase

Single Image Wavefront Sensing Using AI Based Phase Retrieval

Wyant College of Optical Sciences

University of Arizona, Tucson
September 29th 2022

Dr. Gaston Baudat
Innovations Foresight, LLC

Bio

Born in Lausanne Switzerland along the Geneva's Lake (Switzerland). Received a bachelor's degree in electronics & mechanical engineering from the Lausanne Institute of Technology and a Master's degree in electrical engineering and computer science from the Swiss University for Applied Sciences.

Post graduated in biological and artificial neural network from the Swiss Polytechnical School of Lausanne (EPFL). Received a PhD's degree in computer science in the field of machine learning from the French National Conservatory of Arts and Crafts (CNAM) at Paris.

35 years of experience in opto-electronics, analog/digital sensor, and embedded system designs. Extensive experience in document sensing and pattern recognition algorithms using hyper spectral data, digital image processing, advanced statistics, and AI. Move in the USA an became the senior research director for MEI & CPI (Crane co.), retired now.
Co-founder, owner and current president of Innovations Foresight making innovative technologies and products for astronomy and optics.

Initial Motivation

On site quantitative optical testing & alignment of telescopes under Earth atmospheric turbulences (seeing) limited conditions.

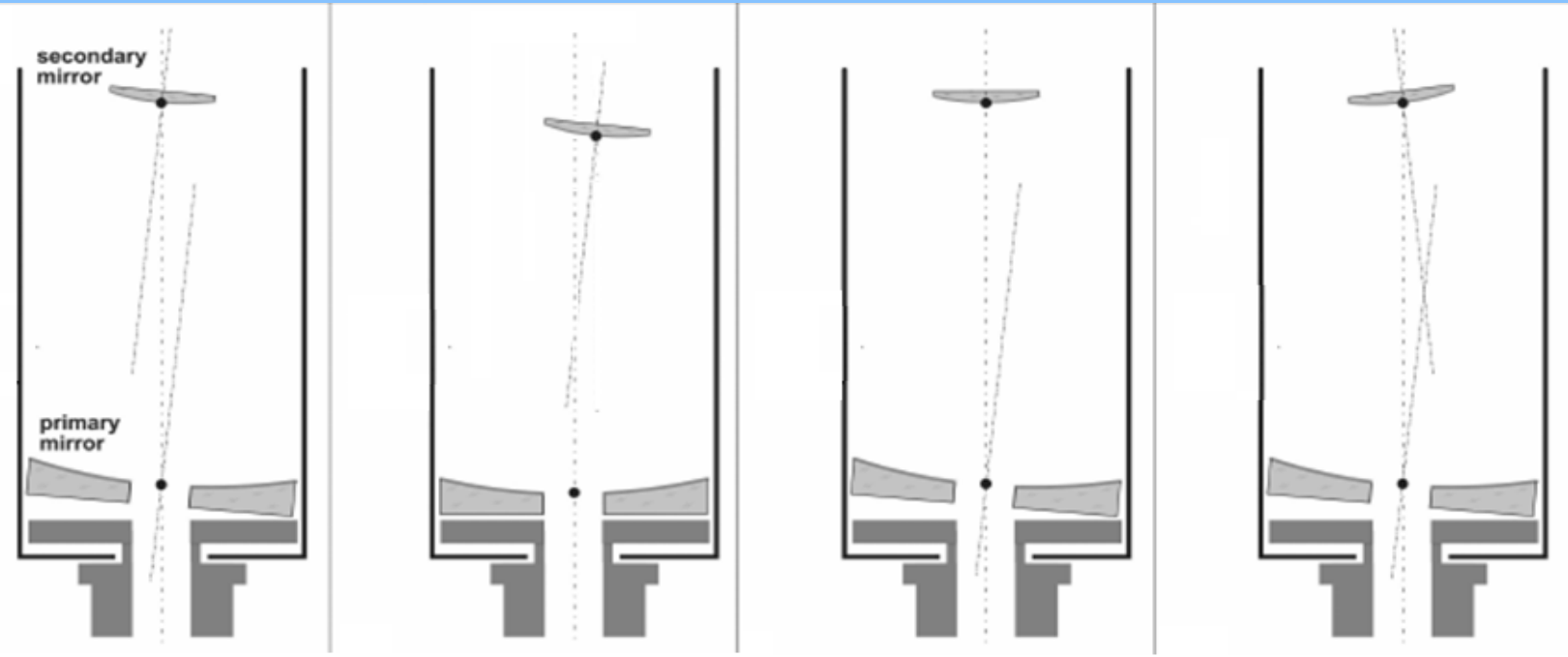

Out of alignment scope: Various misalignment scenarios (reflector)

Key Goals & Objectives

- No extra hardware, use of customer existing camera & focuser.
- Use of actual or artificial stars (temporally incoherent light).
- Works under seeing limited conditions.
- Common-path image-based wavefront sensing.
- High phase dynamic range (no 2π phase wrapping problem).
- Requires only a single image.
- Whole field wavefront (WF) sensing (on and off axis) at once.
- Fast (no iteration, solver, …) at run time, up to 100 fps (AO).

Image Based Wavefront Sensing

Use of the image irradiance (intensity) for phase reconstruction.

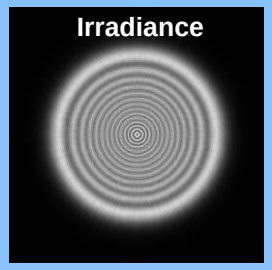

Defocused image (point source)

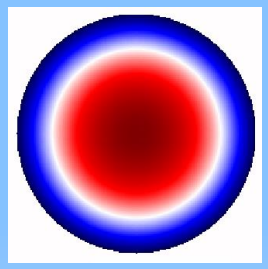

Wavefront phase

$$PSF(u,v) \propto \left|\mathcal{F}\left[p(x,y)e^{j\varphi(x,y)}\right]\right|^2$$
$$PSF(u,v) \overset{?}{\mapsto} \varphi(x,y)$$

- Image based wavefront sensing
  - Non-Parametric
    - Single Image
      - **Phase Retrieval**
      - *- Image space, near to focal plane.*
      - *- Known source.*
      - *- Iterative error reduction algorithms, Gerchberg-Saxton, etc*
    - Multiple Images
      - **Phase Diversity**
      - *- Image space, near to focal plane.*
      - *- Unknow source.*
      - *- Iterative joint maximum a posteriori estimation.*
  - Parametric
    - Two images (intra/extra)
      - **Curvature Sensing**
      - *- Pupil space, far from focal plane.*
      - *- Point source.*
      - *- Iterative irradiance transport equation (Poisson) solver.*

All require iterative numerical optimizations at run time

AI Based Wavefront Sensing
AIWFS

SPIE Photonics Europe 2020 conference, Strasbourg, France

A feedforward neural network (NN) is trained using **only** synthetic (simulated) data. Databases can be arbitrary large. Relevant noises are added (seeing, scattering, speckle, read noise, ...). $z_0 = z_1 = z_2 = 0$.

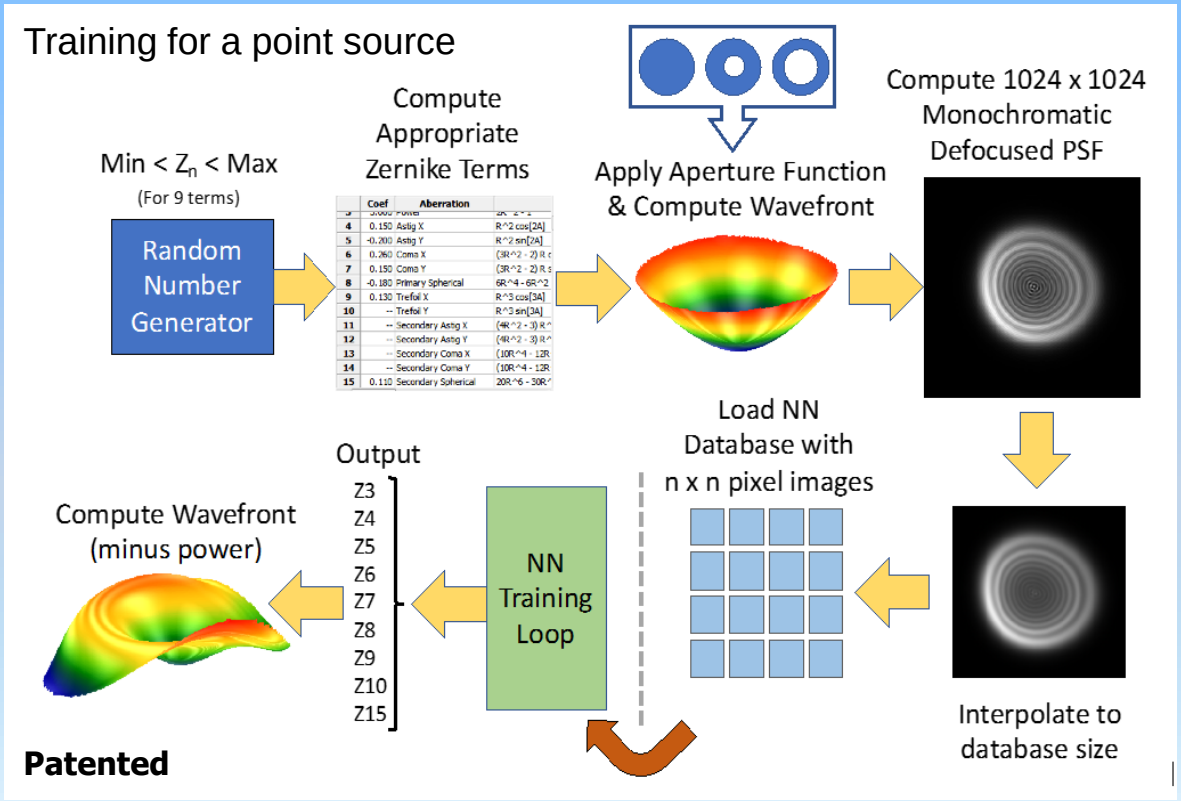

AIWFS: Assumptions & design choices

Telescopes with obscured circular pupils, central obstructions.

Use of annular Zernike polynomials to express the wavefront (balanced aberrations).

Uncoherent light: The piston (Z_0) Zernike polynomial coefficient value is set to zero ($z_0 = o$), there is no global phase shift.

Centered PSF: The x & y tilts (Z_1 , Z_2) polynomial coefficients are set to zero ($z_1 = z_2 = 0$), there is no spatial shift.

In this presentation an in-focus PSF is defined as having no Zernike defocus term, $z_3 = z_2^0 = 0$.

AIWFS: NN Training

The NN is trained to learn the function $h\big(PSF(u,v)\big) = \varphi(x,y)$. The training is done once, beforehand, by minimizing a regularized empirical risk over M learning synthetic samples:

$$\hat{h} = \arg\min_{h \in H} \left\{ \frac{1}{M} \sum_{k=1}^{M} \big(\varphi_k - h(PSF_k)\big)^2 + \gamma \Omega(h) \right\}$$

There is no optimization nor any iteration at run time anymore.

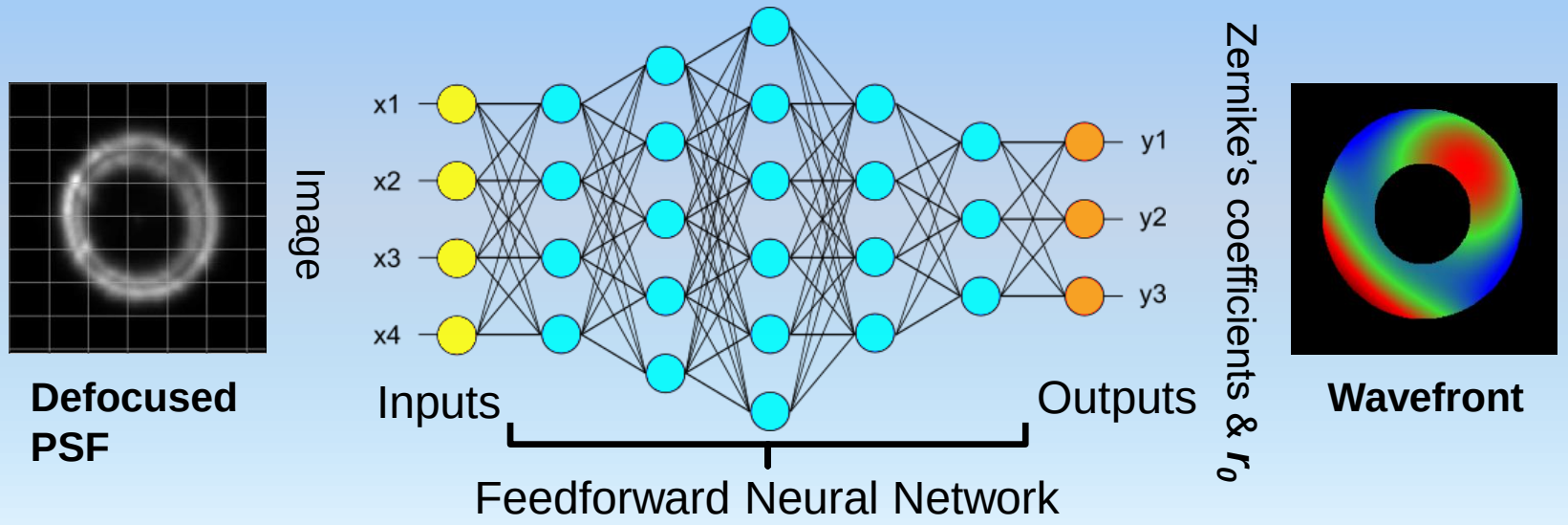

Phase Retrieval and Phase Ambiguity

In-focus PSF:

no aberration	+3 waves Z_8 primary spherical	-3 waves Z_8 primary spherical

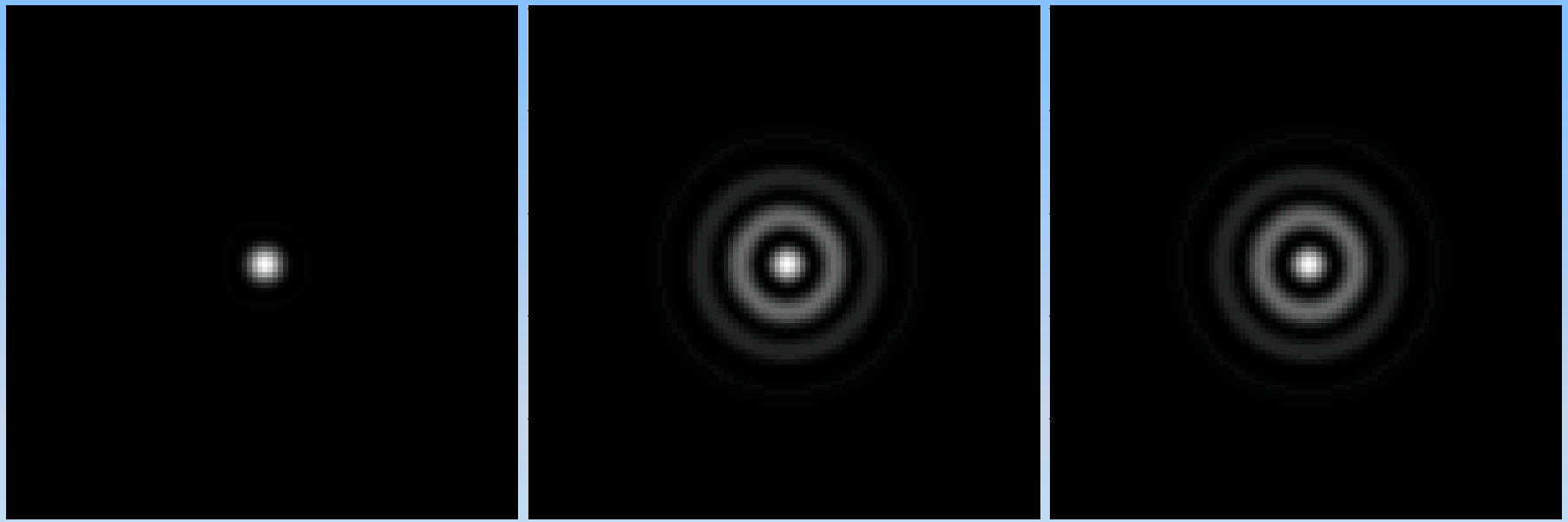

For all 3 PSFs $z_3 = 0$, no defocus (DF)

Uniqueness of Phase Retrieval

Beside global phase (Z_0) & spatial shifts (Z_1, Z_2), phase retrieval faces a last trivial* ambiguity, conjugate inversion, as shown from the pupil function $P(x,y) = p(x,y)e^{j\varphi_p(x,y)}$ cross-correlation, the OTF:

$$OTF(\zeta,\eta) = P(x,y) \otimes P(x,y) = P^*(-x,-y) \otimes P^*(-x,-y)$$

There are 2 pupil functions $\mathrm{P}(x,y)$ leading to the same PSF:

1st $\quad \mathrm{P}(x,y) = p(x,y)e^{j\varphi_p(x,y)}$

2nd (ambiguous) $\quad \mathrm{P}^*(-x,-y) = p(-x,-y)e^{-j\varphi_p(-x,-y)}$ conjugate inversion

For a circular aperture $p(x,y)$ is a real even function, therefore:

$$p(x,y) = p\,(-x,-y)$$

* to avoid non-trivial ambiguities proper FFT sampling is required. (R. H. T. Bates 1982)

Phase Conjugate Inversion Ambiguity

For the pupil phase, its decomposition on odd and even parts shows that ambiguity only exists for its even part.

1st $\varphi_p(x,y) = \varphi_e(x,y) + \varphi_o(x,y)$

2nd (ambiguous) $-\varphi_p(-x,-y) = -\varphi_e(-x,-y) + \varphi_o(x,y)$ conjugate inversion

Example: In-focus PSF with 3rd order balanced spherical & coma.

$z_3 = 0$

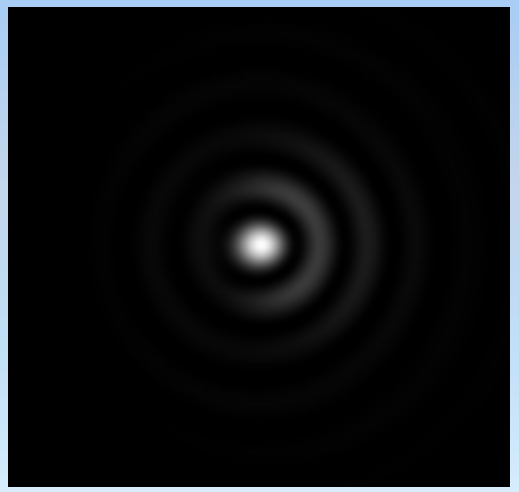

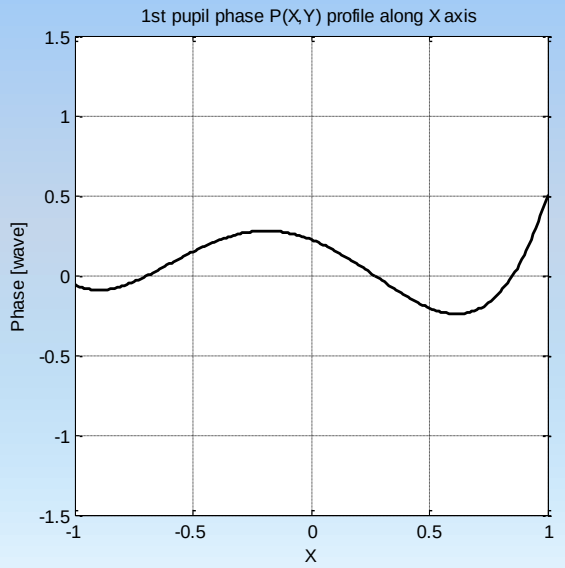

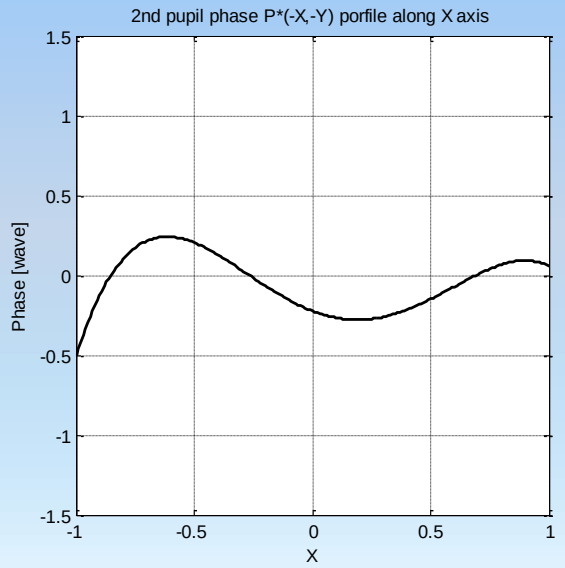

Dealing with Phase Ambiguity

Solution: Add a known defocus (modulation), or bias, $B\varphi_{DF}(x,y)$.

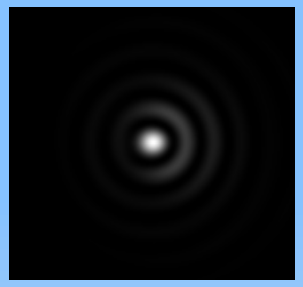

assuming a circular unity pupil ($R = 1$)

$$\varphi_p(x,y) + B\varphi_{DF}(x,y)$$

in-focus, $z_3 = 0$ — defocus bias

$$\varphi_{DF}(x,y) = Circ\left(\sqrt{x^2+y^2}\right)(x^2+y^2)$$

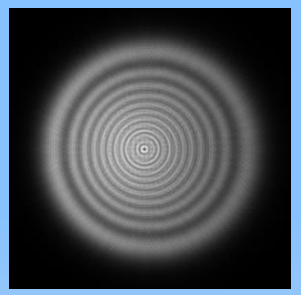

$\varphi_p(x,y)$ is the pupil phase of the in-focus PSF such $z_3 = 0$, B is the defocus bias & ΔB is some defocus error (from any source).

The first biased (defocused) phases $\varphi_B(x,y)$ is given by:

1st $$\varphi_B(x,y) = \varphi_p(x,y) + (B+\Delta B)\varphi_{DF}(x,y)$$

While its conjugate inversion exhibits an opposed bias $(B+\Delta B)$:

2nd (ambiguous) $$-\varphi_B(-x,-y) = -\varphi_p(-x,-y) - (B+\Delta B)\varphi_{DF}(x,y)$$

Minimum Defocus Bias Magnitude

If $B + \Delta B > 0$ there is no conjugate inversion phase ambiguity anymore. $|\Delta B|$ is an application related defocused error budget.

ΔB must include the (on axis) in-focus PSF focus error ($z_3 \neq 0$), the defocus (bias) distance ΔZ error, as well as any off-axis defocus due to field curvature & sensor tilt. To insure $B + \Delta B > 0$ we place a lower limit to the defocus magnitude B:

$$\min(|B|) > \max(|\Delta B|)$$

The ΔB value is output by the NN as any other aberrations.

The defocus distance ΔZ is given by:

$$\Delta Z = B8(1 - \epsilon^2)^{-1}(f\#)^2\lambda$$

Where B is in wave and ϵ the linear central obstruction ratio.

Example of Phase Retrieval With and without a defocus bias B

No defocus $B, \Delta B = 0$:

no aberration

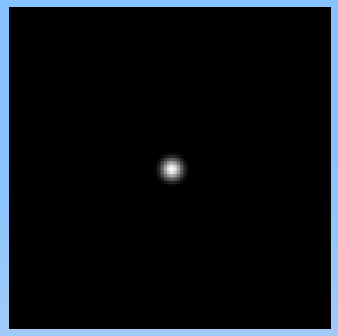

+3 waves Z_8

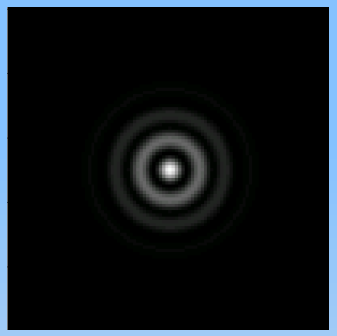

-3 waves Z_8

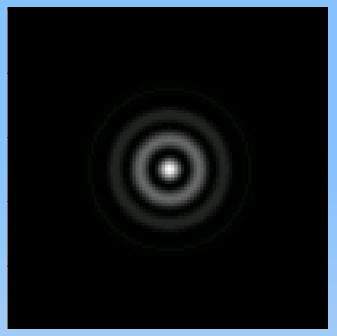

With 10 waves of defocus bias $B > 0, \Delta B = 0$:

no aberration

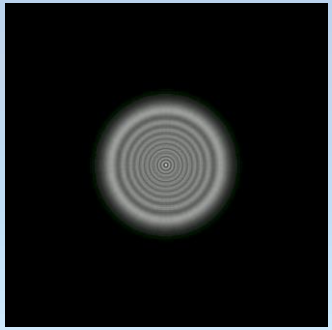

+3 waves Z_8

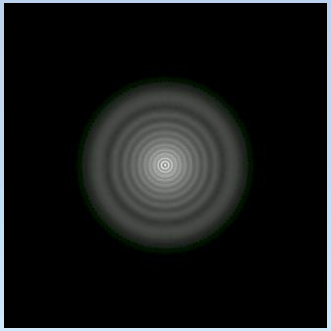

-3 waves Z_8

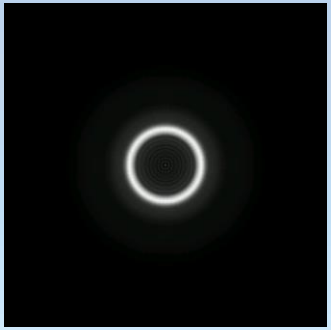

AIWFS: Normalized Data

- To stay generic a single NN is trained using normalized data:

$$R = 1 \text{ and } \lambda = 1$$

- Defocused images are generated from scalar diffraction theory.

Pupil Function $P[k,l]$

$$PSF[m,n] = |FFT_{2D}(P[k,l])|^2$$

$PSF[m,n]$

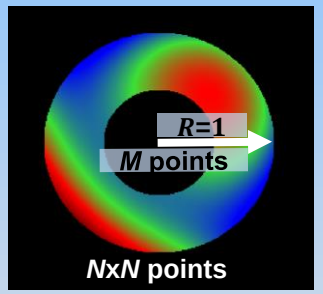

y

x

$$M \in \mathbb{N}^+ \quad N \in 2^{\mathbb{N}^+} \quad N \geq 4M-1 \quad k,l,m,n \in \{-\frac{N}{2}, -\frac{N}{2}+1, \ldots, \frac{N}{2}-1\}$$

$$x = k\Delta s \quad y = l\Delta s \quad u = m\Delta\theta \quad v = n\Delta\theta$$

$$\Delta s = \frac{1}{M} \Rightarrow \Delta\theta = \frac{M}{N}$$

u

v

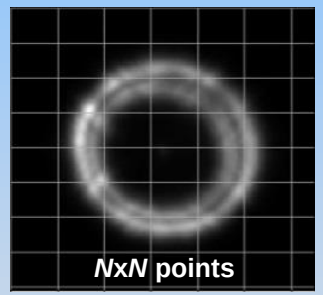

Exit pupil space

Image space

- $\Delta\theta = \frac{M}{N}$ is the simulation normalized PSF sampling period.

Notice: $N \geq 2(2M) - 1$ guarantees no non-trivial phase ambiguity (R. H. T. Bates 1982)

AIWFS: Dealing With Actual optics

Goal: Match the camera images with the NN normalized images.

The NN input images are LxL wide, with $L \leq N$. For a given telescope, at the focal plane, the actual NN pixel size px_{NN} is:

$$px_{NN} = \Delta\theta \frac{N}{L}\frac{\lambda}{R} f = \frac{M}{L}\lambda 2(f\#)$$

Object at infinity with f the effective focal length, R the radius of the exit pupil, with $f \gg \Delta z \Rightarrow f\# \approx constant$

Since the camera pixel size px_C is likely different (often smaller) than px_{NN}. The actual image is resized accordingly before to be fed to the NN.

Example with: $\lambda = 650nm, f/8\,, M = 100, L = 128$

$$px_{NN} = \frac{100}{128} 650 \cdot 10^{-9} \cdot 2 \cdot 8 = 8.13\mu m$$

Portable Test Bench

- Cemented achromat in double pass at f/12.5 (D=24mm).
- Seven 10 μm pinholes (1.5mm pitch) with white LED. For providing field dependent aberration from a single frame.
- 50/50 pellicle beam splitter.
- 16 Mpx (3.8 μm) CMOS camera with red filter in front.

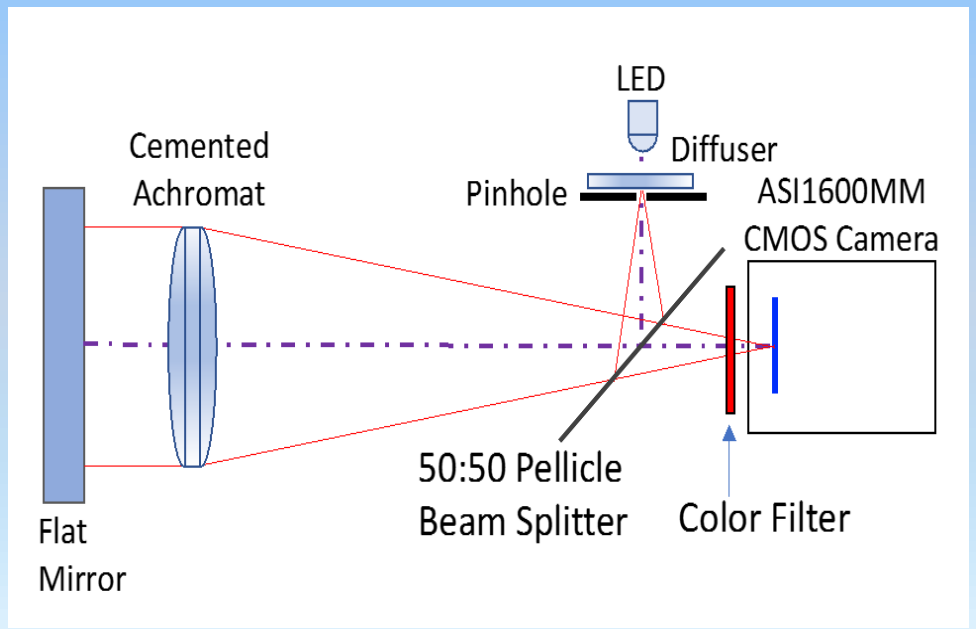

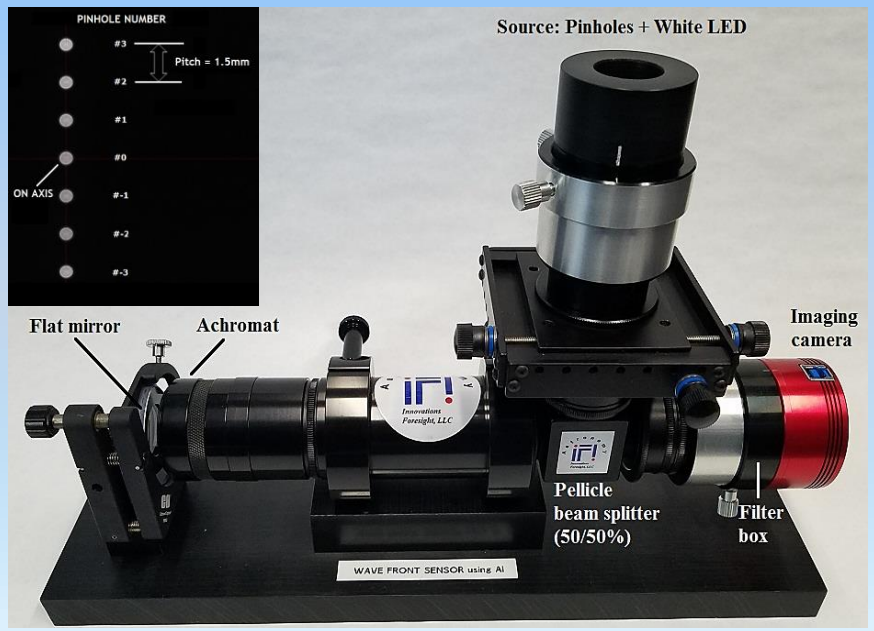

Comparison with a Twyman-Green interferometer

- 4D Technology model 6000 PhaseCam.
- Single-mode stabilized HeNe laser @633nm.
- F/10 diverger lens.

- The ZWO camera + red filter are removed when using the PhaseCam.

AIWFS v.s. PhaseCam on axis flat mirror

SPIE Optical Engineering + Applications 2020 conference, San Jose, CA USA

- 10 micron pinhole, red filter @ 656nm, FWHM = 6nm.
- NN model: 65,536 points (monochromatic extended source). Results in milli-wave [mw].

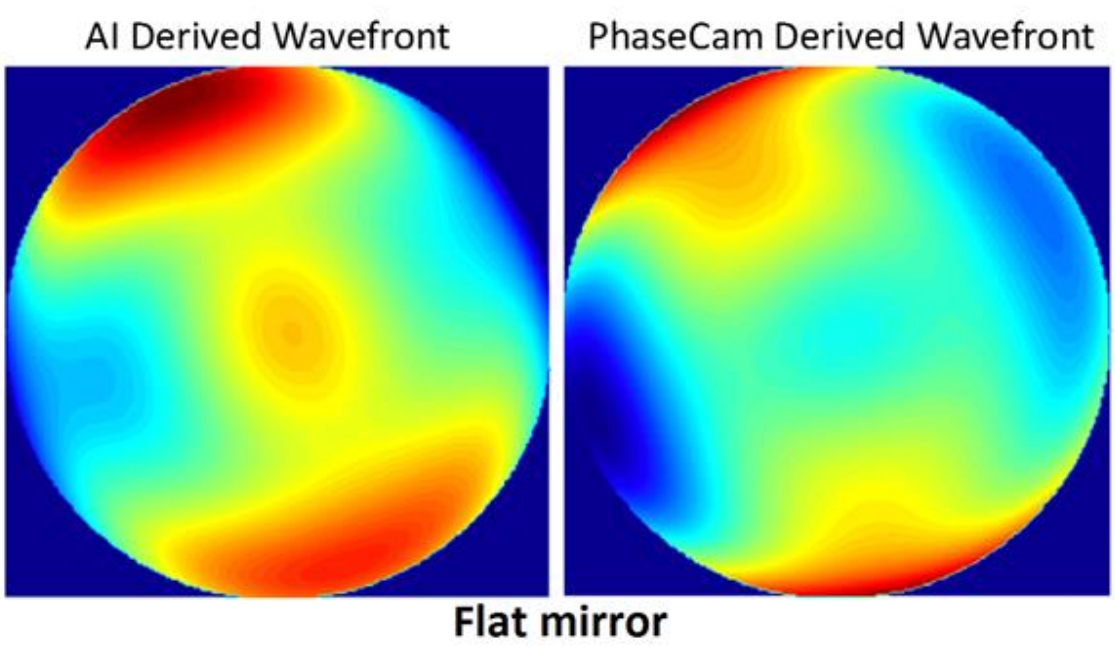

mw	AI	PhaseCam
PV	166	135
rms	27	22
Strehl	97	98
SA3	18	11
CMA3	36	16
ASTG3	-127	-102
Z8	3	2
Z15	16	12
Zernike Trefoil magnitude	14	18

Zernike Wyant's index

Very good agreement, max = 0.025 wave for ASTG3.
Some differences from slight alignment errors & wavelengths.

AIWFS v.s. Shack–Hartmann on axis flat mirror

- Same source, careful alignment SH & AIWFS @ 650nm
- AIWFS exposure time = 10ms, SH = 200ms
- SH v.s. AI Zernike aberration differences:

Wyant's index	SH	AIWFS
SR	0.9864	0.9869
RMS	0.017 wave (11.2nm)	0.018 wave (11.7nm)
PV	0.127 wave (82.2nm)	0.116 wave (75.4nm)
Primary Astigmatism Z4+Z5	0.039 wave (25.0nm)	0.041 wave (26.7nm)
Primary Coma Z6+Z7	0.002 wave (1.5nm)	0.003 wave (2nm)
Primary Trefoil Z9+Z10	0.005 wave (3.5nm)	0.006 wave (3.9nm)
Primary Spherical Z8	0.002 wave (1.4nm)	0.002 wave (1.3nm)
Secondary Spherical Z15	0.021 wave (13.4nm)	0.019 wave (12.4nm)

rms = 0.0014 wave (0.9nm), max = 0.002 wave (1.3nm)

AIWFS versus SH on axis flat mirror

- 3D wavefront plots

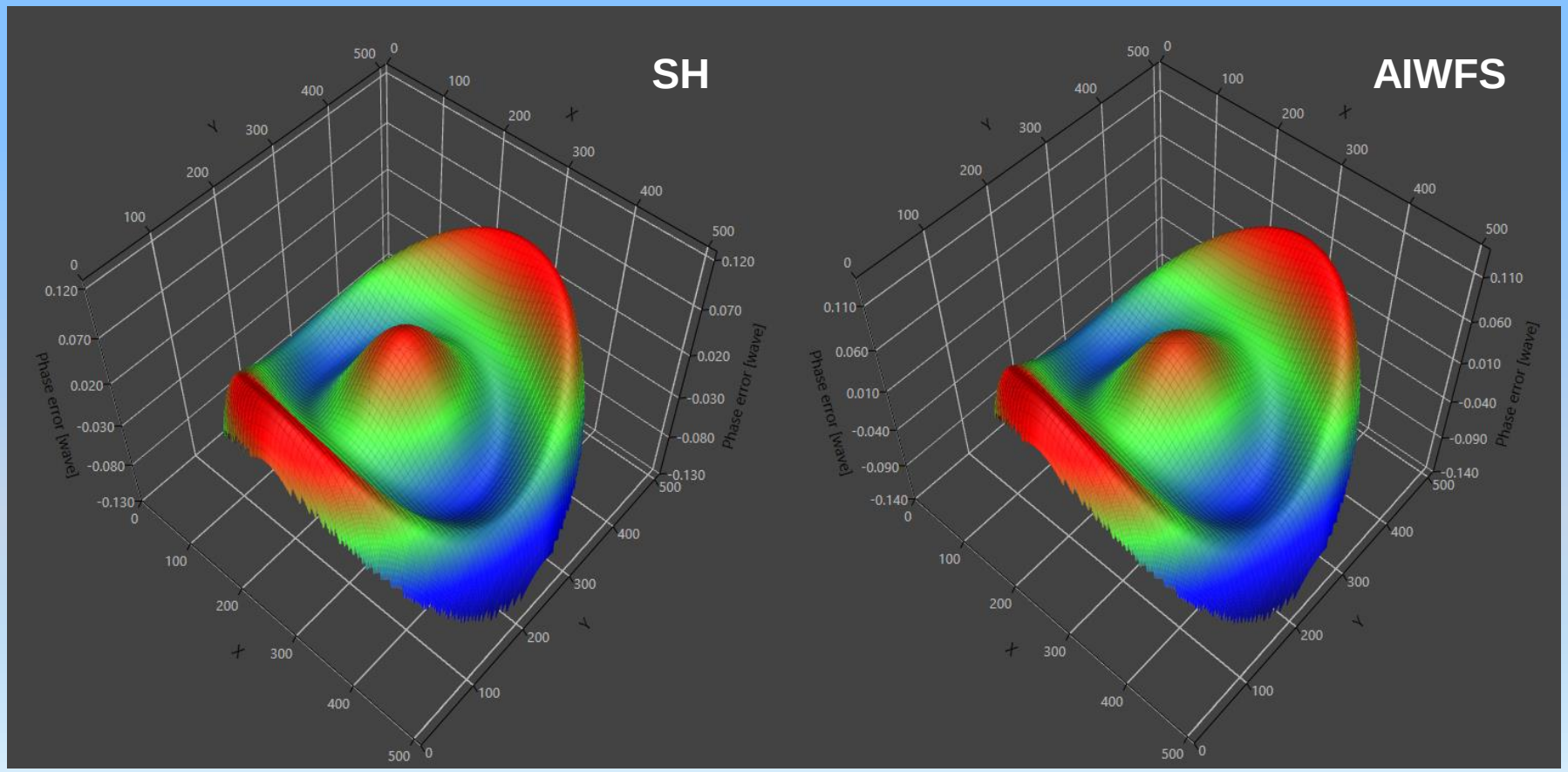

CDK20 Telescope at the Lab

Planewave Instrument 508mm (20”) @ f/6.8 corrected Dall-Kirkham telescope

- 4D technology PhaseCam at the lab, double pass.

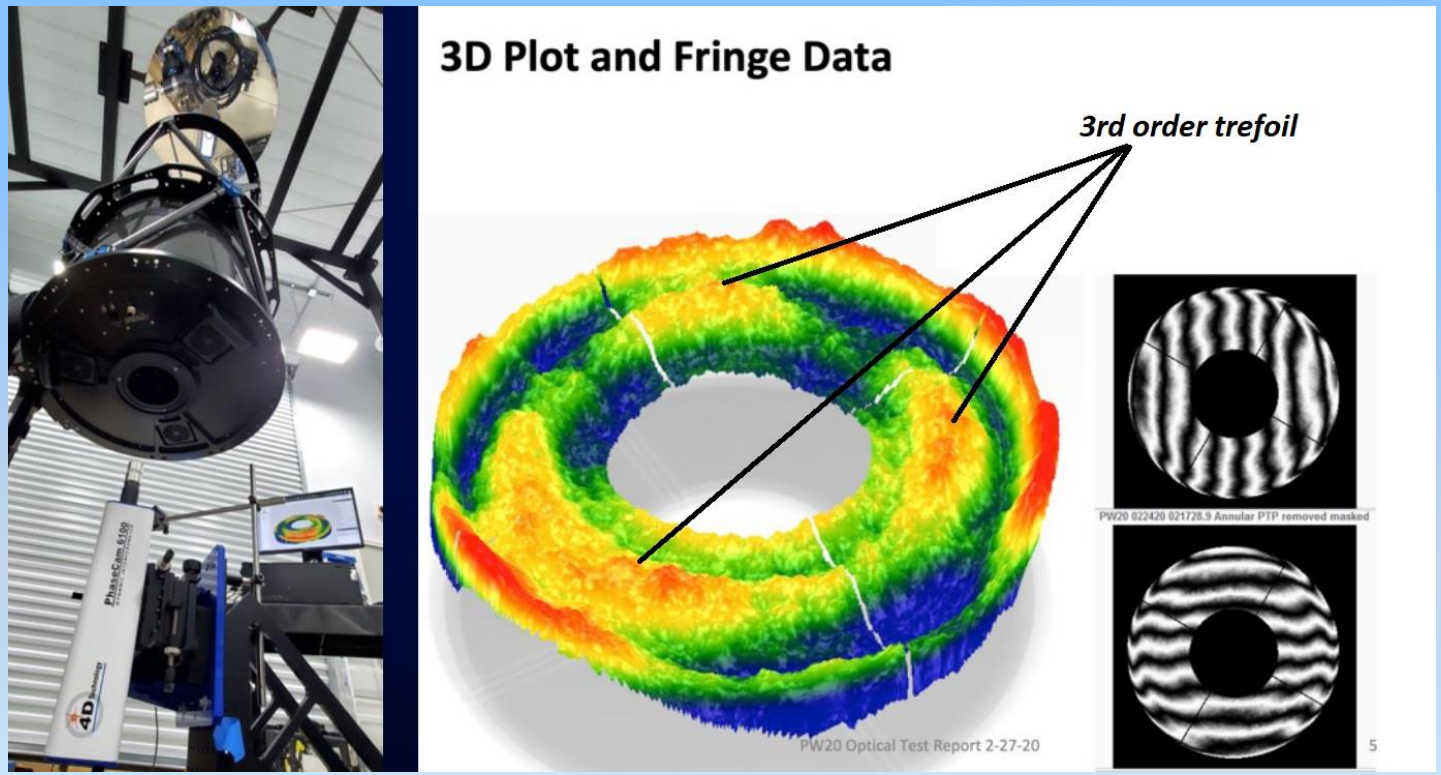

Credit: Dr. John B. Hayes

CDK20 Telescope in the Sky using our AIWFS Technology

- AIWFS in the sky at Bend Oregon, with a red filter, $r_o \cong 8.6\text{cm}$.
- To place in perceptive DL $\Longrightarrow \sim 0.075$ wave rms error.

Credit: Dr. John B. Hayes

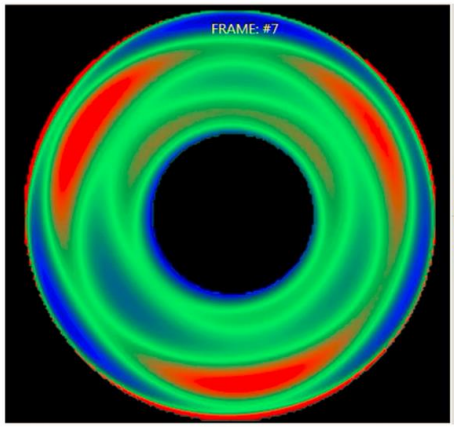

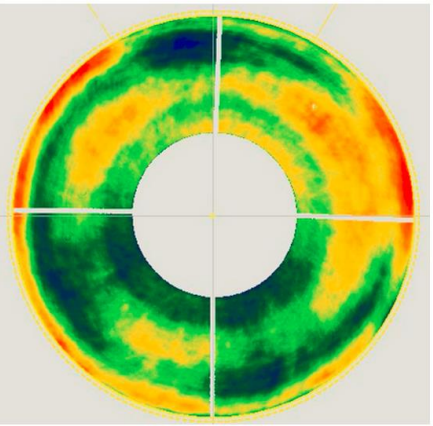

AIWFS (sky)	PhaseCam (lab)
One single frame	**Average 512 frames**
RMS = 0.070 wave	RMS = 0.0647 wave
Measured SR = 0.82	Measured SR = 0.85

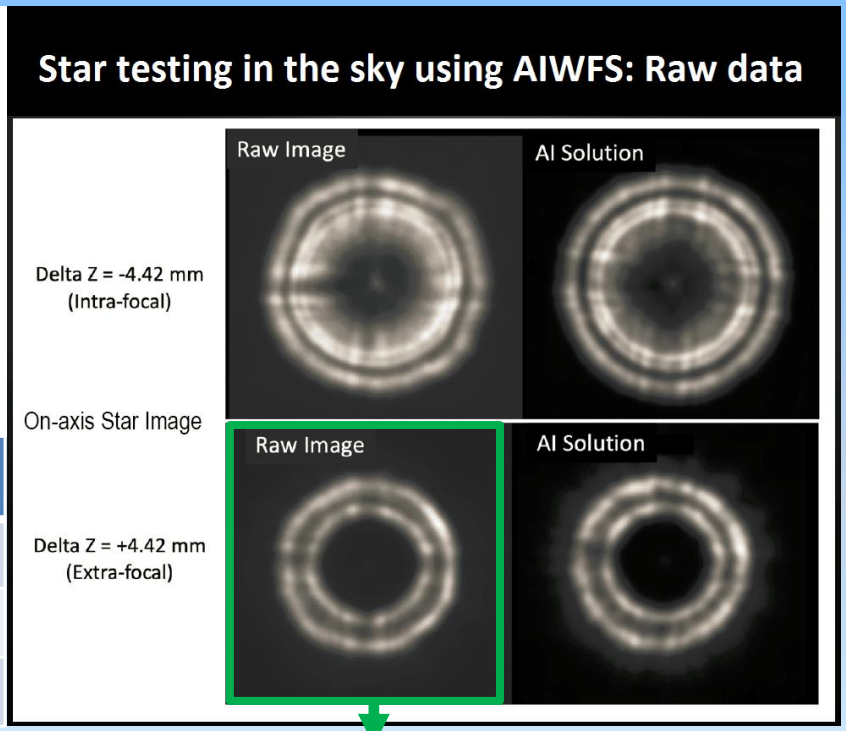

AIWFS v.s. Shack–Hartmann in the sky

- Patrick space force base FL, DOMAS–RGNext, D=559mm, f/9.1
- Exposure time: 5 seconds with red filter @ 656nm, FWHM 6nm
- Seeing estimated at 2.7" (r_0~4.9cm)
- SH v.s. AIWFS annular Zernike aberration differences:

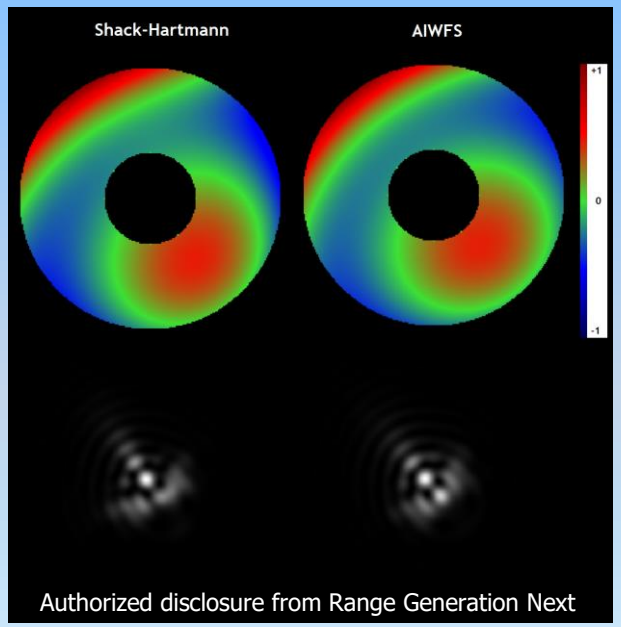

Zernike Wyant's index	SH	AIWFS
SR	0.14	0.19
RMS	0.277 wave	0.271 wave
Astigmatism Z4+Z5	0.96 wave	0.91 wave
Coma Z6+Z7	0.98 wave	0.98 wave
Trefoil Z9+Z10	0.05 wave	0.11 wave
Spherical Z8	0.05 wave	0.11 wave

rms difference = 0.05 wave (0.01 wave rms), max = 0.06 wave

AIWFS
Conclusions

- Single image, low cost, no extra hardware, flexible approach using only synthetic data.
- Fast run time, ~20 fps for 11 Zernike terms on this laptop (256x256 px).
- Whole field wavefront sensing at once, in real time (no extra sensor).
- Can learn and output Zernike coefficients, Fried's parameters, ...
- Large dynamic range and noise tolerant (scattering, speckle, …).
- Access to higher order aberrations (tested up to $Z_{35} = Z_{10}^{0}$ and counting).
- Lab accuracy ~ 0.004 wave rms @650nm.
- Sky accuracy (under seeing limited condition) ~ 0.02 wave rms @650nm.
- Estimated precision (repeatability) ~ 0.002 wave rms @650nm.